 CMC, vol.4, no.1, pp.11-19, 2006

# Elastic Vibration Behaviors Oof Carbon Nanotubes Based on Micropolar Mechanics

**G. Q. Xie**[1,2], **S. Y. Long**[1,3]

**Abstract:** The concept of the micropolar theory is employed to investigate vibration behaviors of carbon nanotubes. The constitutive relation has been deduced from the two-dimensional analysis of the microstructure of the carbon nanotube. Van der Waals interactions are simulated by a weak spring model. Hamilton's principle is employed to obtain dynamics equations of the multi-walled carbon nanotube. Numerical examples for both single-walled and double-walled carbon nanotubes are presented and the significant difference in vibration behaviors between them has been distinguished. Numerical results show that fundamental frequencies for the cantilever single-walled carbon nanotube decreases with increase of the aspect ratio of them, and the fundamental frequencies of the double-walled carbon nanotube are lower than those of the single-walled carbon nanotube with the same inner diameter and length. The first four natural frequencies for the double-walled carbon are coaxial.

**keyword:** Vibration, Carbon nanotubes, Micropolar mechanics, Hamilton's principle

## 1 Introduction

Carbon nanotubes (CNTs) are regarded to be a potential nanostructured material. CNTs possess extraordinary mechanical properties such as extremely high strength, specific stiffness. Besides the promising mechanical properties associated with carbon nanotubes, they also possess excellent thermal and electric properties. Many applications of CNTs have been reported, such as atomic-force microscope (AFM), field emitters (Fan et al. 1999), nano-fillers for composite materials, micro-electronic devices (Yao et al. 1999; Rueckes et al. 2000). Multi-walled carbon nanotubes can be adopted to manufacture nano-devices for instance frictionless nano-actuators, nano-motors, nano-bearings, and nano-springs (Lau 2003).

However, it is necessary to have the fundamental understanding of the nanostructural materials to take advantage of these potential mechanical properties of the carbon nanotube. Dominant methods of the theoretic study on carbon nanotubes are atomistic simulation, continuum model and multi-scale simulation methods. Atomistic simulating techniques are defective for simulation of physical phenomena occurring on a vast range of length scales. The continuum model has become a promising tool for studying CNTs. So far, a few continuum mechanics methods have been adopted by Ru (2001); Li and Chou (2003a); Wang et al. (2005); Qian et al. (2005); Nasdala et al. (2005) to investigate properties of the carbon nanotube. Multi-scale simulation methods are used by Kohlhoff et al. (1991); Gumbsch (1996); Hiroshi Kadowaki and Wing Kam Liu (2005); Shengping Shen and S. N. Atluri (2004) to study nano-mechanics.

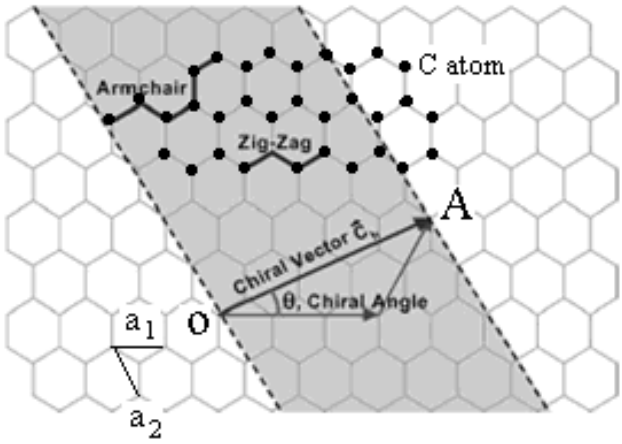


**Figure 1** : Schematic diagram of a regular hexagonal graphene sheet (Thostenson et al., 2001).

Carbon nanotubes (CNTs) are composed of carbon atoms

[1] Department of Engineering Mechanics , Hunan University, Changsha 410082, P.R. China
[2] The Key Laboratory of Advanced Technology for Vehicle Body Design & Manufacture of Ministry of Education, Hunan University, Changsha 410082, P.R. China
[3] Corresponding author

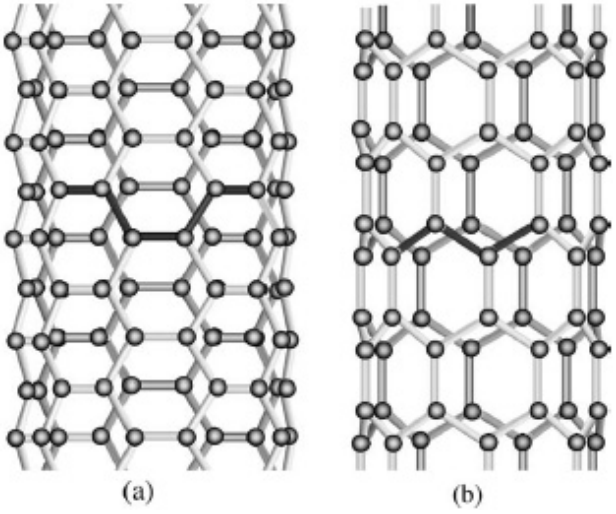


**Figure 2** : Schematic diagram of (a) an armchair and (b) a zigzag nanotube (Thostenson et al., 2001).

which lie on the corner of a regular hexagon (see Fig. 1). A single-walled carbon nanotube (SWNT) is rolled theoretically up with a graphene sheet. Based on their helicity (Dresselhaus M.S. 1997), the fundamental configuration of CNTs can be classified into three categories: armchair, zig-zag, and chiral. And the armchair ($30^o$) and the zig-zag ($0^o$) are the two limit case. SWNT can also be described by the hexagonal base vector $(a_1, a_2)$. To describe this structure, a chiral vector is defined as $OA = na_1 + ma_2$. Its perimeter is $L = a\sqrt{n^2+m^2+nm}$, where $a$ is the length of the base vectors $a_1$ and $a_2$, $a = 0.246$nm, its radius is $d = \frac{L}{\pi}$.

In this paper, constitutive equations of the carbon nanotube are obtained on the basis of the concept of the micropolar mechanics. Hamilton's principle is employed to derive dynamics equations for an element of the carbon nanotube. Governing differential equations are obtained from the assembling of an element matrice by the same way as the finite element method. The first five modal shapes and natural frequencies of the single and double-walled carbon nanotubes have been obtained, respectively. Numerical results show that fundamental frequencies of the double-walled carbon nanotube are lower than those of the single-walled carbon nanotube with the same inner diameter and length. The coaxial vibration of the double-walled nanotube appears at the first four natural frequencies.

## 2 Formulation

### 2.1 Micropolar elasticity theory

The micropolar elasticity theory was adopted by Bazant and Christensen (1972) to analyze the stress field in a cellular solid. In order to obtain the representative elastic modulus for a lattice structure, they developed the finite-difference equation for the struts surrounding a typical node.

In the micropolar elasticity (Eringen 1968; Nowacki 1986; Lakes 1991), the difference of the micropolar continuum from the classical elasticity is the introduction of an additional deformation variable which is the microrotation field. For a planar problem of a microstructured solid, at any point of the solid, a two rank displacement and rotation vector are denoted by **u** and $\phi$, respectively, relative to a Cartesian coordinate system **x**.

### 2.2 Strain-displacement relations

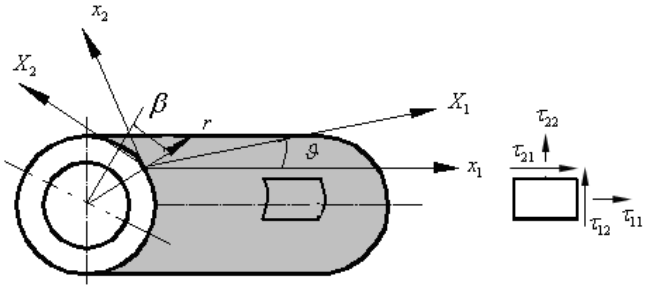


**Figure 3** : The coordinates of the carbon nanotube and the component of stresses

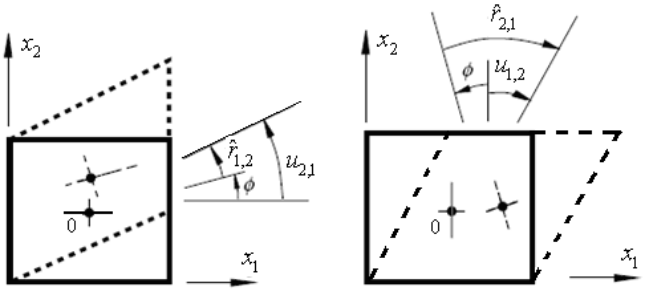


**Figure 4** : Displacement gradient $u_{i,j}$, microrotation $\phi$ and relative deformation $\hat{\gamma}_{i,j}$. The dashed lines represent the deformed state

Figure 3 shows the coordinates of the carbon nanotube. Figure 4 shows the deformation of a unit cell. Based on

the micropolar elasticity, strain-displacement relations of the carbon nanotube are given as

$$\varepsilon_{11} = \frac{\partial u_1}{\partial x_1} \tag{1}$$

$$\varepsilon_{22} = \frac{1}{R}\frac{\partial u_2}{\partial \beta} - \frac{u_3}{R} \tag{2}$$

$$\varepsilon_{12} = \varepsilon_{21} = \frac{1}{2}\left(\frac{1}{R}\frac{\partial u_1}{\partial \beta} + \frac{\partial u_2}{\partial x_1}\right) \tag{3}$$

$$\omega = \frac{1}{2}\left(\frac{\partial u_2}{\partial x_1} - \frac{1}{R}\frac{\partial u_1}{\partial \beta}\right) \tag{4}$$

$$\hat{\gamma}_{12} = \varepsilon_{12} + (\omega - \phi) \tag{5}$$

$$\hat{\gamma}_{21} = \varepsilon_{21} - (\omega - \phi) \tag{6}$$

$$\hat{\phi}_{13} = \phi_{,1} \tag{7}$$

$$\hat{\phi}_{23} = \phi, 2 \tag{8}$$

where a comma denotes partial differentiation with respect to the subsequent spatial coordinate; $\hat{\gamma}_{12}$ and $\hat{\gamma}_{21}$ are relative distortions; $\hat{\phi}_{13}$ and $\hat{\phi}_{23}$ are microrotation gradients; $\omega$ is macrorotation; $R$ is the inner radius of the carbon nanotube.

### 2.3 *Stresses and strains under the different coordinate systems*

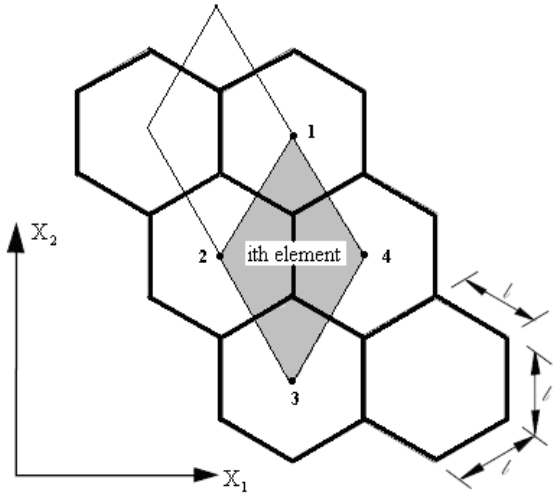


**Figure 5** : Geometry of a regular hexagonal graphene sheet and its*i*th element

The bond between two carbon atoms in the carbon nanotube are regarded as a strut, The carbon nanotube is composed of a regular distribution of similar hexagonal cells. In order to obtain the constitutive relation for the carbon tube, a representative element is shown in Figure 5 where the element is marked by the shaded area. The center point of the element is denoted by 0, and the middle points of struts are denoted by small letters $a$, $b$, $a'$, $b'$.

Length, thickness, inertia of each strut is assumed to be invariable, and denoted $l$, $h$ and $I_s$, respectively. Young's modulus of the carbon nanotube is denoted $E_s$.

For stress and strain analysis, it is necessary to define the stress and strain under the different coordinate system and to to derive their transformation relationships. A system of the natural coordinate is arranged with axes $x_1'$, $x_2'$ that are parallel to sides of the unit cell as shown in figure 6. The tractions have tangent components $\sigma_{12}'$, $\sigma_{21}'$ and normal component $\sigma_{11}'$. The reference Cartesian coordinate is arranged with the axis $X_1$ that has a angle $\psi = 60^o$. The global coordinate is arranged with the axis $x_1$ that is parallel to the axis of the carbon nanotube. The transformation of the natural coordinates into the global ones can be accomplished by

$$\begin{aligned}\left(x_1', x_2'\right)^T &= \begin{bmatrix} 1 & \mathrm{ctg}\psi \\ -1 & \mathrm{ctg}\psi \end{bmatrix} (X_1, X_2)^T \\ &= \begin{bmatrix} 1 & \frac{\sqrt{3}}{3} \\ -1 & \frac{\sqrt{3}}{3} \end{bmatrix} \begin{bmatrix} \cos\vartheta & \sin\vartheta \\ -\sin\vartheta & \cos\vartheta \end{bmatrix} (x_1, x_2)^T \end{aligned} \tag{9}$$

where $\vartheta$ is the angle of the direction $X_1$ with respect to the direction $x_1$ (see Fig. 3).

Tractions on this unit cell can thus be expressed by the stress tensors in the global coordinate reference frame as

$$\left.\begin{aligned} \sigma_{ij}' &= \sigma_{i'j'} = \ell_{i'i}\sigma_{ij}\ell_{jj'} = \ell_{i'i}e_{il_1}\tau_{l_1l_2}e_{l_2j}\ell_{jj'} \\ m_{i3}' &= m_{i'3} = \ell_{i'i}m_{i3} = \ell_{i'i}e_{il_1}\overline{m}_{l_13} \end{aligned}\right\} \\ l_1, l_2, i', j', i, j = 1, 2 \tag{10}$$

where $\ell_{kp} = \cos\left(x_k', X_p\right)$, $e_{l_1l_2} = \cos\left(X_{l_1}, x_{l_2}\right).\tau_{l_1l_2}$ is the stress tensor in the global coordinate, and $\overline{m}_{l_13}$ is the couple stress tensor in the global coordinate.

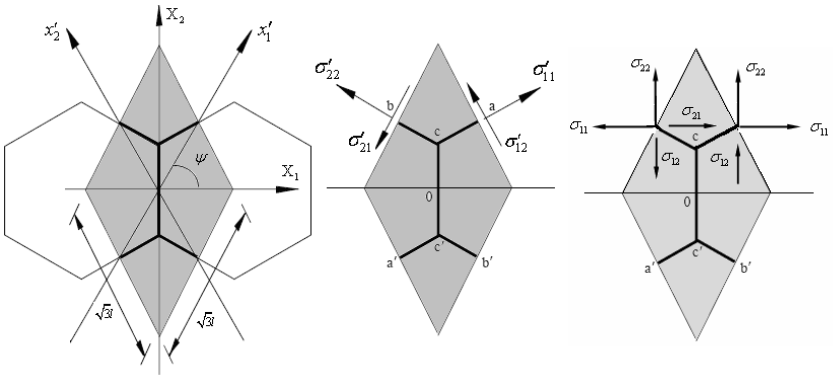


**Figure 6** : Unit cell with natural coordinates $x_1'$, $x_2'$, global coordinates $X_1$, $X_2$ and tractions on the cell sides.

The distortion components of the unit cell are given as

$$\begin{aligned}\varepsilon_{11} &= \frac{\partial u_1}{\partial x_1'}\frac{\partial x_1'}{\partial x_1} + \frac{\partial u_1}{\partial x_2'}\frac{\partial x_2'}{\partial x_1} \\ &= \left(\cos\vartheta - \frac{\sqrt{3}}{3}\sin\vartheta\right)\frac{(u_{1a}-u_{1a'})}{\sqrt{3}l} \\ &- \left(\cos\vartheta + \frac{\sqrt{3}}{3}\sin\vartheta\right)\frac{(u_{1b}-u_{1b'})}{\sqrt{3}l}\end{aligned} \tag{11}$$

$$\begin{aligned}\varepsilon_{22} &= \frac{\partial u_2}{\partial x_1'}\frac{\partial x_1'}{\partial x_2} + \frac{\partial u_2}{\partial x_2'}\frac{\partial x_2'}{\partial x_2} \\ &= \left(\frac{\sqrt{3}}{3}\cos\vartheta + \sin\vartheta\right)\frac{(u_{2a}-u_{2a'})}{\sqrt{3}l} \\ &+ \left(\frac{\sqrt{3}}{3}\cos\vartheta - \sin\vartheta\right)\frac{(u_{2b}-u_{2b'})}{\sqrt{3}l}\end{aligned} \tag{12}$$

$$\begin{aligned}\hat{\gamma}_{12} + \phi = u_{2,1} &= \frac{\partial u_2}{\partial x_1'}\frac{\partial x_1'}{\partial x_1} + \frac{\partial u_2}{\partial x_2'}\frac{\partial x_2'}{\partial x_1} \\ &= \left(\cos\vartheta - \frac{\sqrt{3}}{3}\sin\vartheta\right)\frac{(u_{2a}-u_{2a'})}{\sqrt{3}l} \\ &- \left(\cos\vartheta + \frac{\sqrt{3}}{3}\sin\vartheta\right)\frac{(u_{2b}-u_{2b'})}{\sqrt{3}l}\end{aligned} \tag{13}$$

$$\begin{aligned}\hat{\gamma}_{21} - \phi = u_{1,2} &= \frac{\partial u_1}{\partial x_1'}\frac{\partial x_1'}{\partial x_2} + \frac{\partial u_1}{\partial x_2'}\frac{\partial x_2'}{\partial x_2} \\ &= \left(\frac{\sqrt{3}}{3}\cos\vartheta + \sin\vartheta\right)\frac{(u_{1a}-u_{1a'})}{3l} \\ &+ \left(\frac{\sqrt{3}}{3}\cos\vartheta - \sin\vartheta\right)\frac{(u_{1b}-u_{1b'})}{3l}\end{aligned} \tag{14}$$

$$\begin{aligned}\hat{\phi}_{13} = \phi_{,1} &= \frac{\partial \phi}{\partial x_1'}\frac{\partial x_1'}{\partial x_1} + \frac{\partial \phi}{\partial x_2'}\frac{\partial x_2'}{\partial x_1} \\ &= \left(\cos\vartheta - \frac{\sqrt{3}}{3}\sin\vartheta\right)\frac{(\phi_{1a}-\phi_{1a'})}{\sqrt{3}l} \\ &- \left(\cos\vartheta + \frac{\sqrt{3}}{3}\sin\vartheta\right)\frac{(\phi_{1b}-\phi_{1b'})}{\sqrt{3}l}\end{aligned} \tag{15}$$

$$\begin{aligned}\hat{\phi}_{23} = \phi,2 &= \frac{\partial \phi}{\partial x_1'}\frac{\partial x_1'}{\partial x_2} + \frac{\partial \phi}{\partial x_2'}\frac{\partial x_2'}{\partial x_2} \\ &= \left(\frac{\sqrt{3}}{3}\cos\vartheta + \sin\vartheta\right)\frac{(\phi_{1a}-\phi_{1a'})}{3l} \\ &+ \left(\frac{\sqrt{3}}{3}\cos\vartheta - \sin\vartheta\right)\frac{(\phi_{1b}-\phi_{1b'})}{3l}\end{aligned} \tag{16}$$

### *2.4 Stress-strain relationship of the carbon nanotube*

Based on the symmetry of the cell, the problem can be simplified. It is necessary for the derivation of the constitutive relation to calculate the nodal displacements. This is accomplished by the structural analysis described by Wang and Stronge (1999).

#### *2.4.1 Normal stresses*

This case is shown as figure 7a, where only normal stress $\sigma_{11}$ and $\sigma_{22}$ are applied. In view of Eq. (10), for combined flexure and stretching under these forces the corresponding nodal displacements are

$$u_{1a} = (\cos\vartheta)\,\hbar_{1a} + (\sin\vartheta)\,\hbar_{2a} \tag{17}$$

$$u_{1b} = (\cos\vartheta)\,\hbar_{1b} + (\sin\vartheta)\,\hbar_{2b} \tag{18}$$

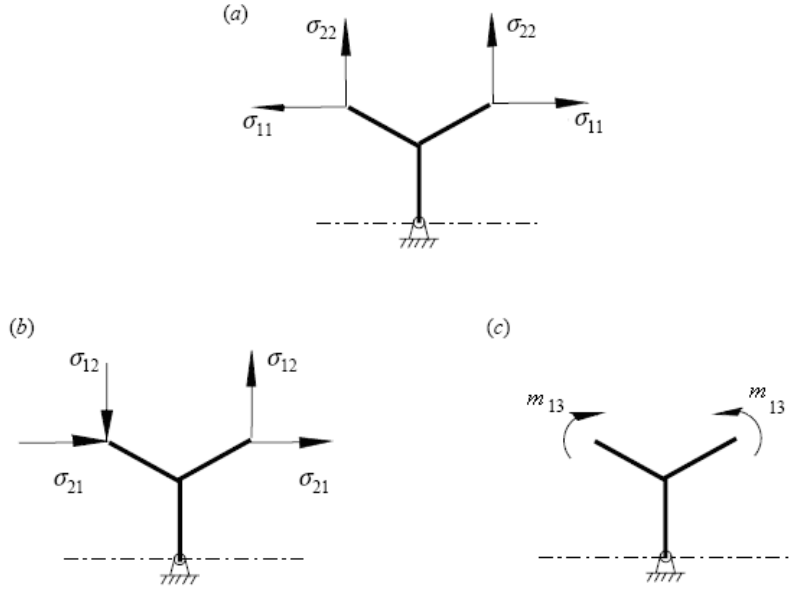


**Figure 7** : Unit cell subjected to stress resultants that are: $(a)$ symmetrical; $(b)$ anti-symmetrical; $(c)$ symmetrical. (Wang X.L., Stronge W.J. 1999)

$$u_{2a} = (-\sin\vartheta)\,\hbar_{1a} + (\cos\vartheta)\,\hbar_{2a} \tag{19}$$

$$u_{2b} = (-\sin\vartheta)\,\hbar_{1b} + (\cos\vartheta)\,\hbar_{2b} \tag{20}$$

$$\phi = 0 \tag{21}$$

where

$$\hbar_{1a} = \frac{3l\eta}{16E_s}\left[\eta^2\left(\cos 2\vartheta\,(\tau_{11}-\tau_{22}) + \sin 2\vartheta\,(\tau_{12}+\tau_{21})\right) + \tau_{11}+\tau_{22}+2\lambda_1\right] \tag{22}$$

$$\hbar_{2a} = \frac{3\sqrt{3}l\eta}{16E_s}\left[-\eta^2\left(\cos 2\vartheta\,(\tau_{11}-\tau_{22}) + \sin 2\vartheta\,(\tau_{12}+\tau_{21})\right) + \tau_{11}+\tau_{22}+2\lambda_2\right] \tag{23}$$

$$\hbar_{1b} = -\hbar_{1a} \tag{24}$$

$$\hbar_{2b} = \hbar_{2a} \tag{25}$$

where $\eta$ denotes the slenderness ratio of the cell wall, $\eta = l/h$

$$\lambda_1 = \cos^2\vartheta\tau_{11} + \cos\vartheta\sin\vartheta\,(\tau_{12}+\tau_{21}) + \sin^2\vartheta\tau_{22}$$

$$\lambda_2 = \sin^2\vartheta\tau_{11} - \cos\vartheta\sin\vartheta\,(\tau_{12}+\tau_{21}) + \cos^2\vartheta\tau_{22}$$

*2.4.2 Shear stresses*

This case is shown in figure 7b, where combined flexure and stretching result in nodal displacements

$$u_{1a} = (\cos\vartheta)\,\Re_{1a} + (\sin\vartheta)\,\Re_{2a} \tag{26}$$

$$u_{1b} = (\cos\vartheta)\,\Re_{1b} + (\sin\vartheta)\,\Re_{2b} \tag{27}$$

$$u_{2a} = (-\sin\vartheta)\,\Re_{1a} + (\cos\vartheta)\,\Re_{2a} \tag{28}$$

$$u_{2b} = (-\sin\vartheta)\,\Re_{1b} + (\cos\vartheta)\,\Re_{2b} \tag{29}$$

$$\phi = \frac{\sqrt{3}\eta^3}{4E_s}\left[\sin 2\vartheta\,(\tau_{22}-\tau_{11}) + \tau_{12} - \tau_{21} + 2\left(\tau_{12}\cos^2\vartheta - \tau_{21}\sin^2\vartheta\right)\right] \tag{30}$$

where

$$\Re_{1a} = \frac{9\sqrt{3}l\eta^3}{16E_s}\left[(\tau_{22}-\tau_{11})\sin 2\vartheta + (\tau_{12}+\tau_{21})\cos 2\vartheta\right] \tag{31}$$

$$\Re_{2a} = \frac{3l\eta}{16E_s}\left[(\tau_{22}-\tau_{11})\sin 2\vartheta + (\tau_{12}+\tau_{21})\cos 2\vartheta\right] \tag{32}$$

$$\Re_{1b} = \Re_{1a} \tag{33}$$

$$\Re_{2b} = -\Re_{2a} \tag{34}$$

#### 2.4.3 Couple stresses

This case is illustrated in figure 7c, where only the couple stress $m_{13}$ is applied. The nodal microrotations are

$$\phi_{1a} = \frac{9}{lE_s}\eta^3\left(\overline{m}_{13}\cos\vartheta + \overline{m}_{23}\sin\vartheta\right)$$

$$\phi_{1b} = -\frac{9}{lE_s}\eta^3\left(\overline{m}_{13}\cos\vartheta + \overline{m}_{23}\sin\vartheta\right) \tag{35}$$

Microrotations due to couple stress $m_{23}$ are obtained as

$$\phi_{1a} = \frac{9\sqrt{3}}{lE_s}\eta^3\left(-\overline{m}_{13}\sin\vartheta + \overline{m}_{23}\cos\vartheta\right)$$

$$\phi_{1b} = -\frac{9\sqrt{3}}{lE_s}\eta^3\left(-\overline{m}_{13}\sin\vartheta + \overline{m}_{23}\cos\vartheta\right) \tag{36}$$

Combining the above expressions, the relationship between strains and stresses for an armchair carbon nanotube is obtained as

$$\begin{pmatrix} \tau_{11} \\ \tau_{22} \\ \tau_{12} \\ \tau_{21} \\ \overline{m}_{13}/l \\ \overline{m}_{23}/l \end{pmatrix} = \frac{\sqrt{3}E_s}{6\eta^3}\begin{bmatrix} \frac{(\eta^2+3)\eta^2}{\eta^2+1} & \frac{(\eta^2-1)\eta^2}{\eta^2+1} & 0 \\ \frac{(\eta^2-1)\eta^2}{\eta^2+1} & \frac{(\eta^2+3)\eta^2}{\eta^2+1} & 0 \\ 0 & 0 & \frac{3\eta^2+1}{\eta^2+1} \\ 0 & 0 & \frac{(\eta^2-1)}{\eta^2+1} \\ 0 & 0 & 0 \\ 0 & 0 & 0 \end{bmatrix}$$

$$\begin{bmatrix} 0 & 0 & 0 \\ 0 & 0 & 0 \\ \frac{(\eta^2-1)}{\eta^2+1} & 0 & 0 \\ \frac{3\eta^2+1}{\eta^2+1} & 0 & 0 \\ 0 & \frac{1}{6} & 0 \\ 0 & 0 & \frac{1}{6} \end{bmatrix}\begin{pmatrix} \varepsilon_{11} \\ \varepsilon_{22} \\ \hat{\gamma}_{12} \\ \hat{\gamma}_{21} \\ \hat{\phi}_{13}l \\ \hat{\phi}_{23}l \end{pmatrix} = \mathbf{D}\varepsilon \tag{37}$$

where $E_s$ is Young's modulus of the carbon nanotube.

The relationship between strains and stresses for a zigzag carbon nanotube is also identical to Eq. (37). The relationship between strains and stresses for the other carbon nanotube can be obtained by combining these equations from Eqs. (17) to Eqs.(36).

### 2.5 Van der waals pressure

If van der Waals pressure at any point between adjacent tubes is assumed to be a linear function of the jump in deflection at that point. $p_{(i+1)i}$ denotes van der Waals pressure on tube $i+1$ due to tube $i$, which is positive inward, is given by Ru (2001)

$$p_{(i+1)i} = c_i\left(u_3^{(i)} - u_3^{(i+1)}\right) \tag{38}$$

where $u_3^{(i)}$ is the (inward) deflection of the $i$th tube, Ru (2002) gives van der Waals interaction coefficient $c_i$

$$c_i = \frac{320(2R_i)}{0.16d^2}\ \mathrm{erg/cm^2} \tag{39}$$

where $d = 0.142$nm, $i = 1, 2, \cdots, N-1$, $R_i$ is the radius of tube $i$.

Combination of Eq. (38) and Eq. (39) yields

$$p_{(i+1)i} = -\frac{R_i}{R_{i+1}}p_{i(i+1)} \tag{40}$$

## 3 Finite element formulations

The finite element method approximates the behavior of a continuum by subdividing the body into a finite number of elements, the shaded part in figure 5 shows an element. Each element is connected to its neighbors through a set of points or nodes. The displacements and rotations within each element are related to the nodal displacements and rotation by quadratic interpolation functions, that is,

$$\mathbf{u} = \mathbf{Nd} \tag{41}$$

where $\mathbf{u}$ is a vector composed of displacement and rotation field components, $\mathbf{N}$ is the interpolation function matrix and $\mathbf{d}$ is a vector made up of displacements and rotations of nodal points.

Eqs. (1)-(8) can be written as

$$\begin{pmatrix} \varepsilon_{11} \\ \varepsilon_{22} \\ \hat{\gamma}_{12} \\ \hat{\gamma}_{21} \\ \hat{\phi}_{13} \\ \hat{\phi}_{23} \end{pmatrix} = \begin{bmatrix} \frac{\partial}{\partial x_1} & 0 & 0 & 0 \\ 0 & \frac{1}{R}\frac{\partial}{\partial\beta} & -\frac{1}{R} & 0 \\ 0 & \frac{\partial}{\partial x_1} & 0 & -1 \\ \frac{1}{R}\frac{\partial}{\partial\beta} & 0 & 0 & 1 \\ 0 & 0 & 0 & \frac{\partial}{\partial x_1} \\ 0 & 0 & 0 & \frac{1}{R}\frac{\partial}{\partial\beta} \end{bmatrix}\begin{pmatrix} u_1 \\ u_2 \\ u_3 \\ \phi \end{pmatrix}$$

$$= \mathbf{Lu} = \mathbf{LNd} = \mathbf{Bd} \tag{42}$$

Once the carbon nanotube has been subdivided into elements, the governing differential equation for each element can be obtained by Hamilton's principle, which

takes the form

$$\int_{t_0}^{t_1} \delta(P-T)\mathrm{d}t = 0 \tag{43}$$

where the time $t_0$ and $t_1$ are arbitrary, $P$ and $T$ are the potential energy and kinetic energy of an element, respectively.

The potential energy of an element in the absence of body force is given by

$$\begin{aligned} P_e &= \frac{1}{2}\int_{eV} \varepsilon^T \sigma \mathrm{d}V - \int p_{i(i+1)} \mathrm{d}u_3^{(i)} \\ &= \frac{1}{2}\int_{eV} \varepsilon^T \mathbf{D}\varepsilon \mathrm{d}V - \int c_i \mathbf{n}(\mathbf{u}^{(i)} - \mathbf{u}^{(i+1)})\mathrm{d}u_3^{(i)} \\ &= \frac{1}{2}\mathbf{d}^{eT}\left(\int_{eV} \mathbf{B}^T\mathbf{D}\mathbf{B}\mathrm{d}V\right)\mathbf{d}^e \\ &\quad - \int c_i \mathbf{n}\left((\mathbf{N}\mathbf{d})^{(i)} - (\mathbf{N}\mathbf{d})^{(i+1)}\right)\mathrm{d}u_3^{(i)} \end{aligned} \tag{44}$$

where the domain $eV$ denotes volume of the element, and $\mathbf{n} = [0,0,1,0]$.

The kinetic energy of the element is expressed in terms of the displacement vector as

$$T_e = \frac{1}{2}\int_{eV} \dot{\mathbf{d}}^{eT}\mathbf{N}^T\mathbf{\Lambda}\mathbf{N}\dot{\mathbf{d}}^e \mathrm{d}V \tag{45}$$

where

$$\mathbf{\Lambda} = \begin{bmatrix} \rho & 0 & 0 & 0 \\ 0 & \rho & 0 & 0 \\ 0 & 0 & \rho & 0 \\ 0 & 0 & 0 & \rho J \end{bmatrix} \tag{46}$$

$\rho$ the mass density of the carbon nanotube, $J$ is micro-inertia.

Substituting Eq.(34) and (35) in Eq. (33) and taking variation with respect to $\mathbf{d}^e$ leads to the following governing differential equation of an element

$$\mathbf{K}^e\mathbf{d}^e + \mathbf{M}^e\ddot{\mathbf{d}}^e = \mathbf{q}^e \tag{47}$$

where $\mathbf{q}^e$ is the coupled term of the adjacent carbon nanotube wall due to van der Waals interaction, element stiffness matrix is given as

$$\mathbf{K}^e = \int_{eV} \mathbf{B}^T\mathbf{D}\mathbf{B}\mathrm{d}V \tag{48}$$

And the element mass matrix as

$$\mathbf{M}^e = \int_{eV} \mathbf{N}^T\mathbf{\Lambda}\mathbf{N}\mathrm{d}V \tag{49}$$

Assembling the mass and stiffness matrix of all the elements for the carbon nanotube, the governing equation can be obtained as

$$\mathbf{K}\mathbf{d} + \mathbf{M}\ddot{\mathbf{d}} = \mathbf{0} \tag{50}$$

where $\mathbf{K}$, $\mathbf{M}$ is the total stiffness and mass matrix, respectively.

It is noted that the terms $\mathbf{q}^e$ in Eq. (47) is incorporated into $\mathbf{K}$ when the stiffness matrix of all the elements are assembled.

## 4 Numerical examples and conclusions

In the subsequent numerical examples, assuming $E_s =$ 1TPa, $\rho = 1300\mathrm{kg}/\mathrm{m}^3$ (Hernandez et al., 1998, Salvetat et al., 1999), wall thickness of a single nanotube layer is 0.066nm.

The first five modal frequencies of the single-walled and double-walled carbon nanotubes with different diameters and lengths are obtained in table 1. It can be found from table 1 that fundamental frequencies of both single-walled and double-walled carbon nanotubes are very high and are in the level of terahertz. The fundamental frequency rapidly decreases with the increase of nanotube length. The fundamental frequency of the double-walled carbon nanotube is lower than that of a single-walled carbon nanotube with the same inner diameter. In addition, frequencies for the first two vibrational modes are nearly equal for both single-walled and double-walled nanotubes. We also found the phenomenon which dispersion curve of wave in a carbon nanotube for the first and second mode lap over when we studied on the wave behaviors of carbon nanotube. These results are in accordance with the reference (Li and Chou 2003b).

Fig. 8 shows the first five modal shapes of a single-walled carbon nanotube, the first modal shape is similar to the second one but the direction is opposite. This verifies the above conclusion. The modal shape of a single-walled carbon nanotube is varied with its length and diameter.

Fig. 9 denotes the first five modal shapes of a double-walled carbon nanotube, the first four modal shapes are

**Table 1** : First five natural frequencies of these cantilever armchair carbon nanotubes

| (m n) | L | Mode frequency (THz) | | | | |
|---|---|---|---|---|---|---|
| | | 1 | 2 | 3 | 4 | 5 |
| | | Single-walled | | | | |
| (6, 6) | 4.9 | 9.84 | 9.84 | 10.31 | 10.32 | 14.95 |
| (7, 7) | 5.2 | 7.32 | 7.32 | 9.95 | 9.95 | 12.89 |
| (11,11) | 8.2 | 4.17 | 4.17 | 8.85 | 8.85 | 8.95 |
| (13,13) | 9.8 | 2.05 | 2.05 | 5.59 | 5.59 | 5.60 |
| | | Double-walled | | | | |
| (6, 6)/ (11,11) | 4.9 | 9.12 | 9.12 | 10.08 | 10.08 | 15.74 |
| (7, 7)/ (12,12) | 5.2 | 7.25 | 7.25 | 9.86 | 9.86 | 14.68 |
| (11, 11)/ (16,16) | 8.2 | 3.04 | 3.05 | 7.72 | 7.72 | 11.89 |
| (13, 13)/ (18,18) | 9.8 | 0.93 | 0.93 | 4.37 | 4.37 | 9.88 |

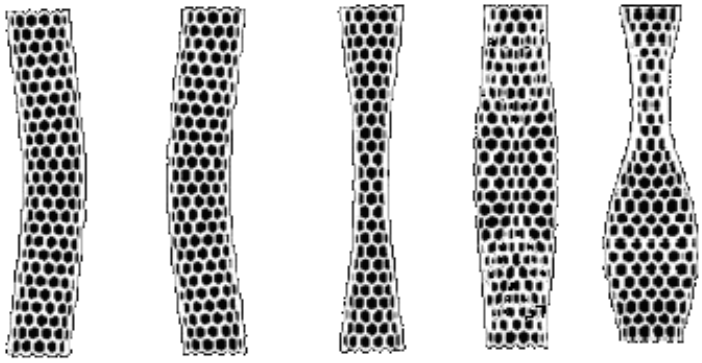


**Figure 8** : First five vibration modal shapes of a cantilever single-walled carbon nanotube.

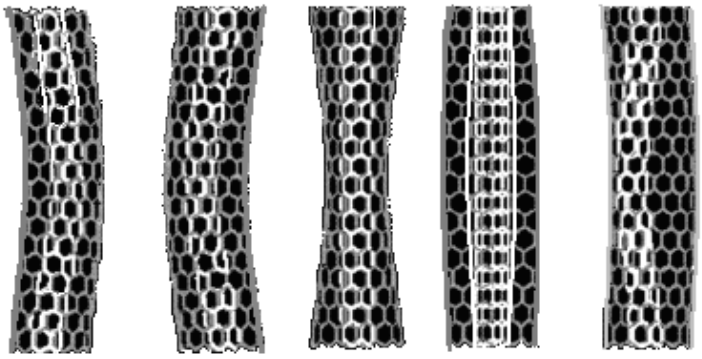


**Figure 9** : First five vibration modal shapes of a cantilever double-walled carbon nanotube.

almost coaxial. It can be found from table 1 that the fifth modal frequency is much higher than the first four modal frequencies, the fourth modal frequency is the critical frequency. The result coincides with the reference (Yoon et al. 2003).

These numerical results show that micropolar theory can also be employed to analyze the mechanics behaviors of nanostructure. The micropolar mechanics demand the

fewer elements than the molecular structural mechanics, and its computational time is shorter than the molecular structural mechanics. The theory possesses the advantages of the classical continuum mechanics, and takes into account the micro-deformation.

**Acknowledgement:** This work is supported by the National Science Foundation of China under the grant number 10372031.

## References

**Bazant, Z.P. and Christensen, M.** (1972): Analogy between micropolar continuum and grid framework under initial stress. *International Journal of Solids and Structure*, Vol. 8, pp. 327 -346

**Dresselhaus M.S.** (1997): Future directions in carbon science. *Annual Review of Material Science*, Vol. 27, pp. 1-34

**Fan, S.; Chapline, M.G.; Franklin, N.R.; Tombler, T.W.; Cassell, A.M.; Dai, H.** (1999): Self-oriented regular arrays of carbon nanotubes and their field emission properties. *Science*, Vol. 394, pp. 52-55.

**Gumbsch, P.** (1996): An atomistic study of brittle fracture: toward explicit failure criteria from atomistic modeling. *Journal of Material Resource*. Vol. 10, pp. 2897-2907.

**Hernandez E.; Goze C.; Bernier P.; Rubio A.** (1998): Elastic properties of C A and $B_xC_yN_z$ composite nanotubes. *Physical Review Letter*. Vol. 80, pp. 4502-4505

**Kadowaki Hiroshi; and Liu Wing Kam** (2005): A multiscale approach for the micropolar continuum model, *CMES: Computer Modeling in Engineering & Sciences*, Vol. 7, No. 3, pp. 269-282

**Nasdala L.; Ernst G.; Lengnick M. and Rothert H.** (2005): Finite Element Analysis of Carbon Nanotubes with Stone-Wales Defects, *CMES: Computer Modeling in Engineering & Sciences*, Vol. 7, No. 3, pp. 293-304

**Lau, K. T.** (2003): Interfacial bonding characteristics of nanotube / polymer composites. *Chemical Physics Letters*, Vol. pp. 370, 399-405.

**Li, C. Y. and Chou T. W.** (2003a): Elastic moduli of multi-walled carbon nanotubes and the effect of van der Waals forces. *Composites Science and Technology*. Vol. 63, pp. 1517–24.

**Li, C. Y. and Chou T. W.** (2003b): Vibrational behaviors of multiwalled-carbon-nanotube- based nanomechanical resonators. *Applied Physics Letters*. Vol. 84, pp. 121-123

**Ru, C.Q.** (2000): Column buckling of multiwalled carbon nanotubes with interlayer axial displacements. *Physics Review B* 62, pp. 16962-16967.

**Ru, C.Q.** (2001): Axially compressed buckling of a doublewalled carbon nanotube embedded in an elastic medium. *Journal of Mechanics and Physical Solids*, Vol. 49, pp. 1265–1279.

**Rueckes, T.; Kim, K.; Joselevich, E.; Tseng, G.Y.; Cheung, C. L.; Lieber, C.M.** (2000): Carbon nanotube-based nonvolatile random access memory for molecular computing. *Science*. Vol. 289, pp. 94-97.

**Salvetat JP, Briggs GAD, Bonard JM, Bacsa RR, Kulik AJ, Stockli T,ET AL.** (1999): Elastic and shear moduli of single-walled carbon nanotubes. *Physical Review Letter*. Vol. 82, pp. 944 -947.

**Shen, Shengping; Atluri, S. N.**. (2004):Computational Nano-mechanics and Multi-scale Simulation, *CMC: Computers, Materials, & Continua*, Vol. 1, No. 1, pp. 59-90

**Thostenson, E.T.; Ren, Z.; Chou, T. W.** (2001): Advances in the science and technology of carbon nanotubes and their composites: a review. *Composites Science and Technology*, Vol. 61, pp. 1899–1912.

**Wang X.L.; Stronge W.J.** (1999): Micropolar theory for Two-dimensional stresses in elastic honeycomb. *Proc.R.Soc.Lond. A* 455, pp. 2091-2116.

**Yao, Z.; Postma, H. W. C.; Balents, L.; Dekker, C.** (1999): Carbon nanotube intramolecular junctions. *Nature,* Vol. 402, pp. 273-276

**Yoon, J.; Ru, C. Q. and Mioduchowski, A**. (2002). Sound wave propagation in multiwall carbon nanotubes. *Phys. Rev. B* 66, pp. 4801-4806.